UNIVERSITÀ DEGLI STUDI DI PADOVA

DIPARTIMENTO DI INGEGNERIA
DELL'INFORMAZIONE

CORSO DI LAUREA IN INGEGNERIA INFORMATICA

Tesi di Laurea

Telecomunicazioni multimodali in reti subacquee: simulazioni ed esperimenti sul campo

Multimodal telecommunications in underwater networks: simulations and on-field experiments

Relatore: Prof. Damiano Varagnolo
Correlatore: Dr. Filippo Campagnaro
Laureando: Davide Pontini

Anno Accademico 2023/2024
Data di laurea: 24/09/2024

Abstract

Research in the field of underwater networks is spreading rapidly: clusters of sensors can be used for monitoring water chemistry and temperature, marine species, energy resources and much more. Nodes need to communicate with each other; however electromagnetic waves, which are used in wireless transmissions on the surface, cannot travel useful distances underwater. Therefore, depending on the purposes and environmental conditions, other modes of information transmission can be used.

This paper illustrates the main advantages and challenges of radiofrequency, acoustic and optical underwater communication, indicating some use cases where they are best suited. Radiofrequency and optical communication can both achieve a very high datarate. However, the former has a very short range due to a strong channel attenuation, and is subject to interference of nearby radios; on the other hand, optical signals are disturbed by sunlight, and require a line of sight to operate. Compared to these technologies, acoustics suffers from long delays and a low bitrate, but its range can be much longer, depending on the frequencies employed.

We carried out some simulations using the C++ libraries of the DESERT framework, made available by the SIGNET research group at the University of Padua. These simulations focus on observing the performance of the different technologies, in various scenarios. We considered channel attenuation and geometrical parameters, like the position and orientation of the nodes, and present the results in the form of plots.

We then conducted an experiment in the Piovego river in Padua, using two proprietary acoustic modems, in order to observe the maximum bitrate achievable at a very short distance. Software-defined modems were used, connected to the DESERT protocol stack on a laptop, so that we could quickly switch between modulations. We tested different datarates by employing different modulations: the most promising ones appeared to be a BPSK modulation, with 10 samples per symbol, and a BPSK at 20 SPS, the latter one adopting OFDM modulation.

Sommario

La ricerca nel campo delle reti sottomarine si sta diffondendo rapidamente: cluster di sensori possono essere utilizzati per monitorare le caratteristiche chimiche e la temperatura dell'acqua, le specie marine, le risorse energetiche e molto altro ancora. I nodi necessitano di comunicare

tra loro; tuttavia le onde elettromagnetiche, utilizzate nelle trasmissioni wireless in superficie, non possono percorrere distanze utili sott'acqua. Pertanto, a seconda degli scopi e delle condizioni ambientali, possono essere utilizzate altre modalità di trasmissione delle informazioni.
Questo paper illustra i principali vantaggi e le sfide della comunicazione subacquea a radiofrequenza, acustica e ottica, indicando alcuni casi d'uso in cui essi sono più adatti. Le radiofrequenze e la comunicazione ottica possono entrambe raggiungere una velocità di trasmissione dati molto elevata. Tuttavia la prima tecnologia ha un range molto breve a causa della forte attenuazione del canale, ed è soggetta ad interferenze causate da dispositivi radio nelle vicinanze; d'altra parte, i segnali ottici sono disturbati dalla luce solare e richiedono una linea di vista per funzionare. Rispetto a queste tecnologie, l'acustica soffre di lunghi ritardi e di un bitrate basso, ma la sua portata può essere molto più lunga, a seconda delle frequenze impiegate.

Abbiamo effettuato alcune simulazioni utilizzando le librerie C++ del framework DESERT, messe a disposizione dal gruppo di ricerca SIGNET dell'Università di Padova. Queste simulazioni si concentrano sul confronto tra le prestazioni delle diverse tecnologie, in vari scenari. Abbiamo considerato l'attenuazione del canale e alcuni parametri geometrici, come la posizione e l'orientamento dei nodi. Presentiamo i risultati sotto forma di grafici.

Abbiamo poi condotto un esperimento presso il fiume Piovego a Padova, utilizzando due modem acustici dell'Università, in modo da osservare il massimo bitrate ottenibile a brevissima distanza. Sono stati utilizzati modem di tipo "software-defined", collegati allo stack di DESERT su un laptop, in modo da poter passare rapidamente da una modulazione all'altra. Abbiamo testato diverse velocità di trasmissione dati impiegando diverse modulazioni: quelle più promettenti sembravano essere una modulazione BPSK, con 10 campioni per simbolo, e una BPSK a 20 SPS, quest'ultima comprendente la modulazione OFDM.

Contents

Introduction

The need for flexible and agile underwater free-space communication is now more evident than ever before. Water masses are rapidly changing, as a result of climate change: temperature and chemical pollution of water, the struggle of many marine species, and the occasional oil or gas spills are phenomena that need to be monitored closely, in order to have an accurate representation of the global scenario, and to be able to intervene quickly when possible.

In many cases, the deployment of multiple sensors on free-roaming drones in an area is an effective approach. However, this requires an efficient way for these nodes to exchange data with each other and with the surface. The water medium presents unique challenges to physical communication, as opposed to air: parameters like water salinity, temperature, ambient light, pressure, turbulence and turbidity all affect data throughput. Furthermore, these parameters can change quickly, requiring dynamic models that can adapt and adjust for offering optimal performance as often as possible.

This paper presents an overview of the main characteristics and challenges of acoustic, optical and radio frequency underwater communications; an acoustic experiment in a short range, fresh water scnenario is also presented and analyzed. The paper is structured as follows: a brief overview of the technologies currently used in underwater networks is presented; for each of them, their known strengths and shortcomings are described. In the following section we illustrate some simulations carried out using the DESERT Framework: they show the performance of acoustic, optic and radio communications when dealing with different water conditions (represented by specific parameters) and with various positions and orientation of the nodes. Graphs are reported to show the packet delivery ratio in the conditions mentioned above, so that results can be compared.

A real-field experiment is then described. We performed some tests in the Piovego river in Padua, using two acoustic modems positioned at a distance of 10 m from each other. The goal was to maximise the bitrate by employing different modulations. This paper aims to derive adequate conclusions from the simulations and experiment, indicating possible scenarios for future research, in the direction of achieving higher transmission bitrates with acoustics.

1 Discussion and comparison of underwater communications technologies

1.1 Radio frequencies

The use of radio frequencies seems promising: after all, it is the designated mode of wireless communication above the surface. However, the signal experiences strong attenuation underwater. The channel attenuation factor α can be derived from [1]:

$$\alpha = \sqrt{\pi \sigma \mu_0 f} \tag{1}$$

where σ is the water conductivity (in Siemens/meter), f is the frequency (in Hertz) and μ_0 is the permeability (in henry/meter). The electrical conductivity σ depends heavily on water salinity: the conductivity of sea water is 4.3 S/m, whereas that of freshwater usually oscillates from 0.001 to 0.01 S/m[5].

The sea's salinity determines a strong attenuation coefficient that prohibits the use of long range RF in a marine environment. The attenuation is also dependent on the carrier frequency; indeed, only VLF or ELF waves can reach useful depths, carrying however such little information (few characters per minute for ELF) that complex data carrying is made impossible. In addition, transmitting at very-low-frequencies requires large antennas, which are heavy, costly and consume a lot of power; they can be a viable option for military applications, but not so much for civil uses. There is also the issue of interference with nearby radios of submarines.

For very-short-range applications, slim devices with a high carrier frequency can still be utilized. This is the case, for instance, in the context of the Aqua-fi project [2], where a diver with a gateway strapped on his back reaches some underwater mobile devices, which send data via RF to the gateway, to be further forwarded.

Figure 1: theA Aqua-fi system in function.

It is evident that radio frequencies are meant to be used underwater only in very specific use cases, where a very short range is sufficient.

1.2 Acoustics

Communication via acoustic waves is drastically different than RF: the bitrate is generally much lower, since the frequencies do not usually exceed the hundreds of KHz. Also, sound speed in water is in the range of 1500 m/s, while electromagnetic waves move at 225000 km/s: that is a factor of more than a hundred thousand. This entails significant delays, which become an important factor in planning sensor networks.

On the other hand, with acoustics it is possible to reach much higher distances, as the signal does not suffer from an attenuation as severe as with RF. While employing low frequencies (below 20 KHz), it is possible to cover tens of kms[3]. The attenuation depends on distance d and frequency f:

$$A(d,f)_{\text{dB}} = k \cdot 10 \log d + d \cdot a(f) \tag{2}$$

where *a(f)* is the absorption loss, and *k* is the spreading factor. For k=2 we have spherical spreading, where the signal propagates in all directions; for k=1 we have cylindrical spreading, which is an accurate model when the distance (*di*) between the transmitting and receiving nodes is $di > 2d$. In this case the signal is subject to self-interference, due to reflections occurring on the sea surface and on the seabed. This worsens the reception. The practical value set is usually k=1.5, corresponding to a distance for which $d/2 < di < 2d$.

The noise $N(f_c)$ is computed as a sum of various components[4]:

- Turbulence noise, which only affects very low frequencies, below 10 Hz.
- Noise caused by distant ships, which interferes with low frequencies, between 10 Hz and 100 Hz.
- Noise of surface waves, which is the main noise component for frequencies between 100 Hz and 100 kHz.
- Thermal noise, which affects frequencies above 100 kHz.

The overall signal-to-noise ratio is computed as follows [5]:

$$\mathrm{SNR} = 10 \log \left(\frac{P_{\mathrm{TX}}}{N(f_c) \cdot \delta f_c} \right) - A(d, f_c) \tag{3}$$

where P_{TX} is the transmitting power, $N(f_c)$ is the noise as a function of the carrier frequency f_c, and δf_c is the bandwidth.
Depending on the use case, a certain carrier frequency can be chosen in order to minimize noise, while still permitting the required datarate for the specific application. As a matter of fact, acoustic modems are usually classified as follows[5]:

- **Low Frequency (LF) acoustic modems**: with a carrier frequency below 20 KHz, they offer a low bitrate of a few hundreds of bit/s, but a range of tens of kilometers.
- **Medium Frequency (MF) acoustic modems**: their carrier frequency is between 20 and 50 kHz, bringing the bitrate to a few kbps, with a range of a few kilometers. LF and MF modems can be used by the navy for surveillance and Mine Countermeasure (MCM) applications.

- **High Frequency (HF) acoustic modems**: with a carrier frequency above 50 kHz, they can reach more than 100 kbps, although the range is limited to less than a km. They are the smallest and lightest devices, usually mounted on micro AUVs or ROVs and used to send comparatively high speed data to a nearby surface station.

Another important factor to consider is the sound speed (*ssp*) gradient: the variation of the propagation speed along the water column, caused by the falling temperature and rising pressure as we venture deeper in the sea. This strongly affects delays and therefore, collisions and needs to be taken into account. The ssp gradient also changes during the day, as water gets heated by the sun (the so called *"afternoon effect"*).

1.3 Optics

Another option for wireless underwater transmission is optical technology. A LED or laser transmits a signal across the water, reaching a receiver equipped with a photodiode. A simple equation can describe the relationship between transmitting (x) and receiving (y) signal intensities[7]:

$$y = \alpha(h)x + n \tag{4}$$

where h is the channel gain, n is the noise and α is the effective power loss due to effects such as absorption and scattering, as will be discussed shortly.
The best frequency to choose is generally the one that matches the water color, green or blue as it might be: that is the color which is least absorbed by the medium. During the day, in case of intense sunlight, it is also advisable to use ultraviolet light: interference with the sun will then be lower, as its ultraviolet irradiance is quite low when compared to the visible spectrum.

The frequencies used in this case are much higher than with RF: visible light is used, usually in the colors green, blue, violet or ultraviolet, bearing a frequency that goes well into the hundreds of THz. This means, potentially, an extremely high bitrate. Indeed, in the aforementioned Aqua-Fi project, the gateway communicated with the surface using a LED or a laser (depending on the depth), reaching speeds of several Mb/s.

Using light in a free-space underwater environment presents its own challenges. Since it is possible to send data directionally, in a much more precise manner than with acoustics, multipath interference is limited; however since a line of sight (*LOS*) is required, the presence of marine life or other natural obstacles can disturb the transmission.

In these frequencies, a significant source of attenuation is the ambient light, which reduces the signal-to-noise ratio. An experiment with a blue LED transmitter in a fish-tank, conducted at the MORSE Studio lab at Georgia State University[6] showed that path loss increases with the increase of salinity, temperature and, most significantly, with water turbidity. These factors significantly impact the range of transmission, which can reach up to 300 m in ideal conditions[8].

In conclusion, there is not a single technology that can be preferred in every scenario: it is therefore useful to mount on the nodes hardware that enables multimodal communication: depending on the channel conditions and range required, the system should dynamically select the best technology. This functionality also requires MAC and routing layer protocols that can behave differently when a different technology is selected. For instance, in [9, 10, 11] authors prove how an AUV, which needs to retrieve data from many submerged sensors, could use acoustics to locate the nodes, and switch to optical when at a feasable distance, for the actual transfer of data.

In the next section we will illustrate a series of simulations, which exemplify some of the key characteristics of RF, acoustic and optical communications that we described.

2 Simulations

We will now present the results of a series of simulations that have been carried out using the DESERT framework, which will now be described. These simulations highlight some of the features of RF, acoustic and optical communication that have already been illustrated. Our focus is not on the speed of the connection, but rather on its robustness. Various positions of the nodes and water conditions are simulated.

We ran each simulation five times; however, since the models used are deterministic, each run with the same set of parameters yielded the same results, which is why we did not include any confidence intervals in the graphs.

2.1 DESERT Underwater

DESERT Underwater is a set of public C++ libraries that constitute an extension of the NS-MIRACLE simulator, which allows to simulate a network in which each node can have multiple modules in each layer of its protocol stack. DESERT extends these functionalities to support the design and implementation of underwater network protocols.

Before showing the result of our work with the DESERT simulator, we describe briefly its installation process. We worked in a Debian-based Linux virtual machine, specifically Ubuntu 22.04.4 (which can be found **here**). First we installed the necessary dependencies with the following command:

```
sudo apt-get install build-essential autoconf automake libxmu-dev libx11-dev libxmu-dev libxmu-headers libxt-dev libtool gfortran bison flex
```

Then we downloaded the proper folder from GitHub:

```
git clone -b master https://github.com/signetlabdei/DESERT_Underwater.git
```

Finally, we ran the installer with the *./install.sh –wizard* command. More installation details can be found on **this page**.

After installing the software, one can proceed with running some simulations. We will now refer to paths inside the main folder, *DESERT_Underwater*. It is needed to first open a terminal in the *DESERT_buildCopy_LOCAL* sub-folder, and source the environment here (*source .\environment*). Then we can move to the desired folder and run the tcl script with the
ns Example.tcl command.

We examined some scripts in the *DESERT_Framework\DESERT\samples\desert_samples*
sub-folder.

2.2 RF simulations

Firstly we consider a situation where a sink is positioned 1 m above the surface, and a node vertically below it. The carrier frequency is 100 MHz, with a bandwidth of 125 KHz. In these conditions we can achieve 27 kbps, which is considered a large value for underwater communications.

Initially we thought to plot the PDR (packet delivery ratio, computed as the ratio of the received packets / transmitted packets) as a function of: 1) depth of the underwater node; 2) water salinity. However, with each scene parameters, we found that the PDR dropped abruptly at a certain point, from a value of 92.32% down to zero. In this case it is therefore more interesting to plot the maximum depth and the maximum salinity before the PDR drop, as a function of the carrier frequency used.

Firstly the salinity was set to 0, to simulate fresh water. We lowered the frequency from 800 MHz to 200 MHz, to see the maximum useful depth of the underwater node. We expected an inverse proportionality, since lower frequencies are less attenuated by the water medium, as we saw in the previous section.

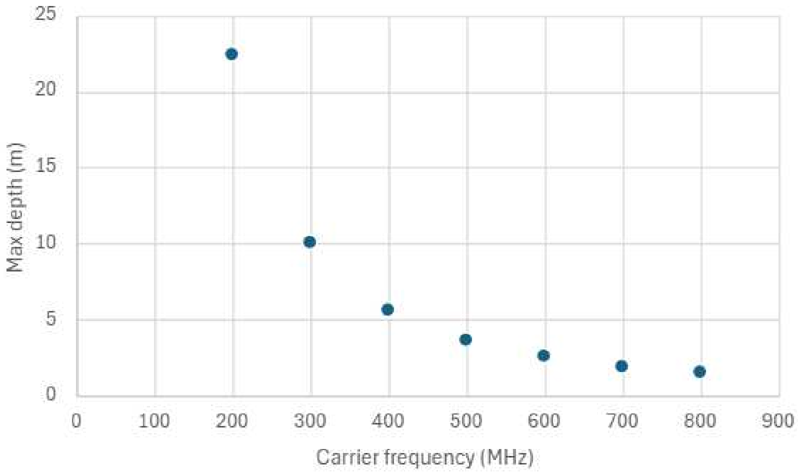

Figure 2: Maximum reception depth at different carrier frequencies of the underwater node.

In theory, a lower frequency requires a bigger and more expensive antenna; however we are here still in the range of the hundreds of MHz, so this is not a significant problem.

We then plotted the maximum salinity that allows reception, with varying carrier frequencies. The depth of the underwater node is now fixed at 1 m.

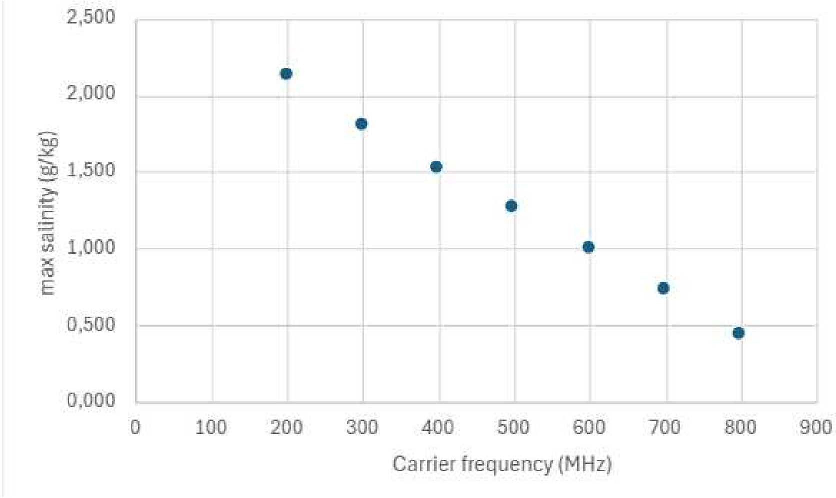

Figure 3: Maximum salinity to have reception, as a function of carrier frequency.

As before, lower frequencies can tolerate a higher attenuation, which is directly correlated with water salinity. It is significant to note that the average salinity of rivers is just 0.12 g/kg, while that of seas and oceans averages 35 g/kg. Lowering the frequency can therefore be useful when a river area is slightly more saline than predicted; this strategy could in theory be used at sea as well, but we measured that the frequency would have to be brought all the way down to 6 MHz, needing an antenna longer than 20 m.

2.3 Acoustic simulations

The simulated scenario contains three nodes in freshwater, all at a depth of 100 m, positioned in a line. The middle node is equidistant from the others. A carrier frequency of 50 kHz and a bandwidth of 36 kHz were used. Spherical spreading is assumed (since the nodes are at a reasonable depth). Firstly we set the windspeed to 10 m/s, and changed the nodes distance from each other (we kept their x and y position at equal values, so that their distance would be $x*\sqrt{2}$). In the graph the distance indicated is the one between the middle node and any of the others.

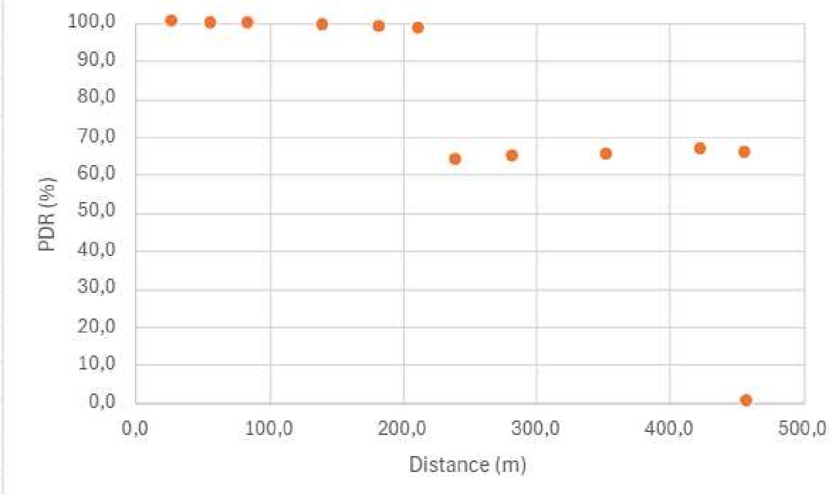

Figure 4: PDR at different nodes positions

As we can see, the PDR is stable at a value close to 100%, up until crossing a distance of 200 m. Then it drops abruptly to a value around 65%, where it stays until the end of the available range. The range is in this case visibly higher than with RF, even though we are using a carrier frequency that is quite high for acoustic communications. At these distances, medium attenuation is not significant. On the other hand, the noise of the surface waves, and therefore the windspeed, can affect the transmission quality. Wind is indeed the main source of noise when transmitting at 50 kHz; the next graph shows its impact on the reception quality, when the fixed position of the nodes is such that the middle one is $100\sqrt{2}$ m from the others:

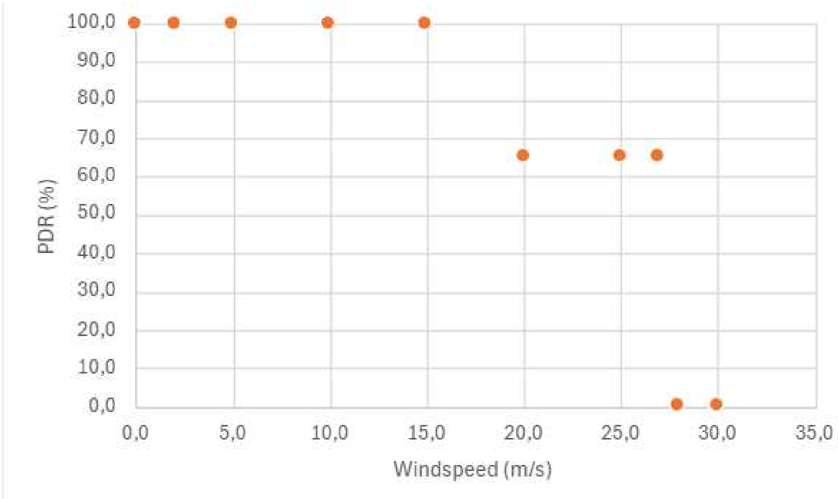

Figure 5: PDR at different values of windspeed

We can observe a similar outline as before, with two stable PDR values and sudden drops.

Noticeably, up until a certain windspeed, we can still receive more than half of the packets, and this ratio could be improved with some retransmission protocol. The maximum speed after which all packets are dropped seems to be 27 m/s, which is the speed of the wind in a storm, that gets a 10 on the Beaufort scale: the connection is therefore robust. Of course, these results depend on the transmission power used. With a power of 160 dB re μPa, the wind noise cannot strongly affect the reception. As a matter of fact, when lowering the power to 150 dB re μPa, the wind plays a more significant role:

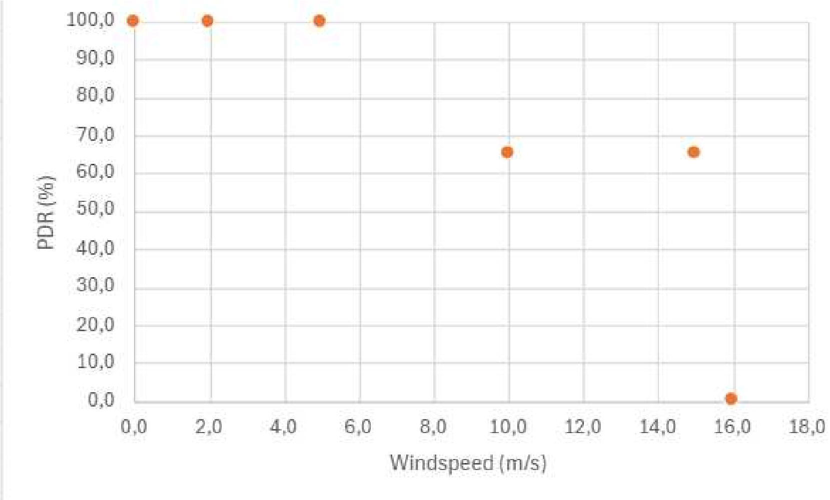

Figure 6: PDR at different values of windspeed. Lower tx power

2.4 Optical simulations

2.4.1 Omnidirectional beam pattern

This scenario is comprised of two nodes, communicating via an optical link in seawater. The two plots we now present are relative to a omnidirectional beam pattern; we will examine a different system afterwards. First we ran a simulation where both nodes are at a depth of 119 m. The following plot shows the PDR against the horizontal distance between them.

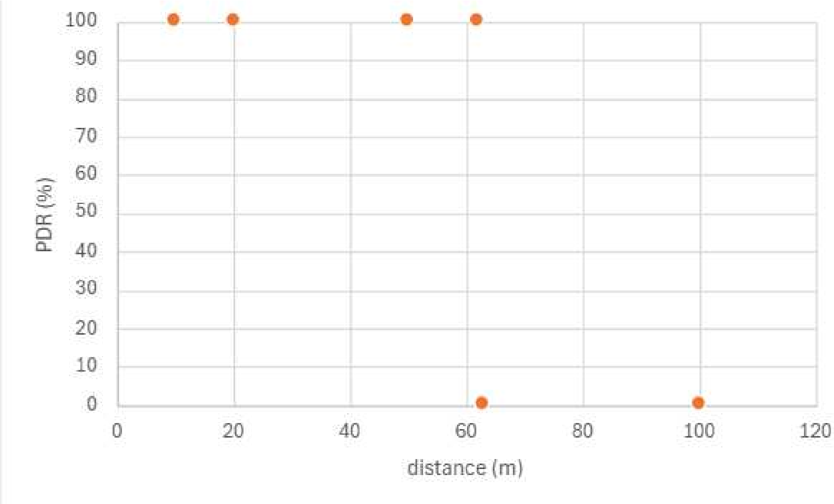

Figure 7: PDR at different distances, using an optical link

The attenuation factor is such that the channel seems to perfectly hold until a distance of 62.846 m; just a millimeter more causes the reception to drop to 0%. This abrupt change is a result of the model employed, but reflects the real experiments quite well, since the goal is usually to maximise the range, even at the cost of risking a sudden stop in the reception of all packets.

The next plot refers to a constant horizontal distance of 10 m between the nodes; one of them is kept at a depth 5 m greater than the other. What is varied is the absolute depth of both nodes, with the shallower one referenced on the x axis.

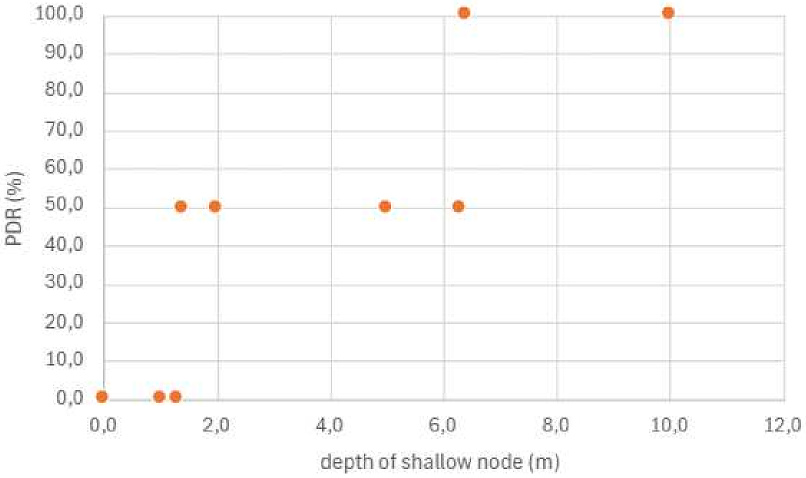

Figure 8: PDR at different depths

We can see two sudden elevations of the PDR: when the nodes are too close to the surface, the sunlight noise makes it impossible to receive anything; starting from a depth of 1.377 m, we have a stable PDR of 49.7%, which then jumps to 100% when the depth reaches 6.334 m.

2.4.2 Real beam pattern

The next two plots refer to a scenario where the model of a realistic optical beam is utilized; this beam pattern is not omnidirectional, so the power received at a certain distance also depends on the orientation of the two nodes. When the only parameter changing is said orientation, we found that the PDR is either 100% or 0%. Instead of having the PDR on the y axis, it is therefore more useful to observe the maximum angle that still allows reception. The first plot below shows this critical angle as a function of the horizontal distance; the depth is kept at 119 m as in the omnidirectional beam case. We are rotating only the left node, keeping the case where the nodes directly face each other as a reference for the null angle. The angles are expressed in degrees.

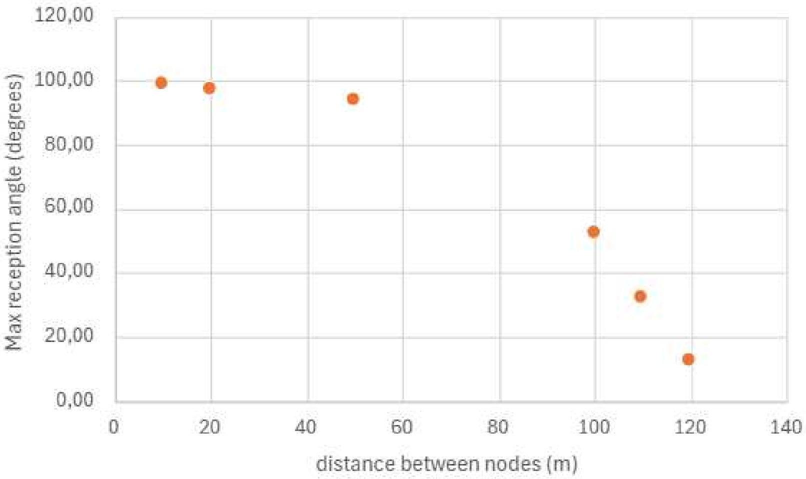

Figure 9: Max angle to receive, at different distances

When the nodes are up to 50 m from each other, reception holds even for an angle greater than $\pi/2$, meaning in a condition where the bulk of the signal is actually not moving towards the receiver, but further from it. On the other hand, a considerable angle of $\pi/4$ still permits reception at distances comparable with the maximum one (126.789 m), achievable for the optimal null angle. This shows that some small rotation, that could be caused by water currents or by the impact with nearby fish, still permits a robust transmission. The range is quite lower than with acoustics, but the frequencies used, and therefore the datarate achievable, is significantly higher.

Lastly, we ran the same simulation as for the case of the omnidirectional beam pattern, where the independent variable is the depth of the nodes. Since the distance between them does not change, the maximum angle is fixed, and has a value of 99° (from the optimal reference of both nodes having vertical orientation, facing each other).

3 Experiment in the Piovego river

In this section we describe the on-field experiment that we performed within the project of this thesis. It involves two acoustic modems, communicating at a very short range. Since the carrier frequency is fixed at 40 kHz, we can change the modulation to achieve different datarates. The goal is to test how high a bitrate the channel can support.

We will briefly describe the modems that we used and the experiment setup. We will then illustrate the results obtained, and suggest some future tests and research that can help deepen our knowledge about similar communication scenarios.

3.1 System description

Both nodes of our network consisted of a modem connected to a laptop on a local IP network. The modem is a Rasberry Pi 4, with a HiFiBerry DAC+ ADC Pro[13] on top of it for signal conversion. The Aquarian Scientific AS-1 transducer is used, with a PA-4 Hydrophone Preamplifier in reception. [12] describes this modem in more detail.
The modem was developed by the University of Padua as part of the MODA project[14]. It is a software-defined modem (SDM): its hardware is not specialized, but is rather composed only of a few processing units. It is therefore reconfigurable: its protocol stack is adaptable to the specific channel environment at hand. This allows for the use of simpler, less expensive and multi-purpose hardware.

A few socket channels connect the SDM to a driver, which makes for a substitute of the physical layer of the DESERT protocol stack on the laptop. This allows the DESERT framework to be used not only for simulations, but for real-field trials as well.

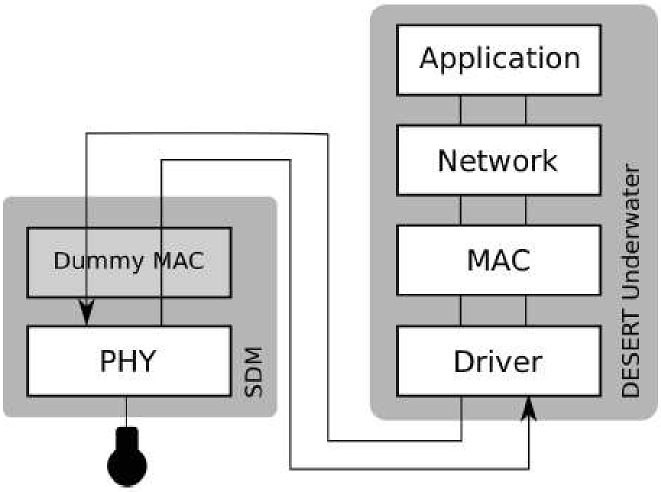

Figure 10: SDM and DESERT protocol stacks.

Through the sockets, the modem sends diagnostics (RSSI, PDR), data and event notifications to the driver, and receives commands to change the configuration scheme based on this information.

Therefore, the two devices work in sinergy: the modem is used to configure different modulation and channel encoding schemes (with constraints related to the physical characteristics of the transducer), while the DESERT software can develop protocols for various layers. The result is a versatile and flexible platform for testing underwater communication in various scenarios.

3.2 Setup and conditions

With the help of the Unipd SIGNET staff, the experiment setup was prepared. The tests were performed in the Piovego River in Padua, a channel presenting weak currents and virtually no shipping noise: since the river is narrow and shallow, only a few small boats occasionally traverse it. One modem was placed on the bridge of Porta Portello, so that the hydrophone could be lowered into the water below, at an approximate depth of 1 m: ideally it should be placed far from the water surface, but the riverbed is only 1.8 meters deep in that point. We conducted the first experiment in the morning, placing the second modem on a nearby dock, at a distance of about 80 m. However, with all the requested modulations, reception was basically inexistent: the Piovego river presents pillars that cause multipath and self-interference, both at the dock and in the middle of the river, in the transmission path. It was not possible to place the hydrophone far enough from the dock to actually see some packet reception.

It is worth to note that the main obstacle in this scenario is indeed the self-interference caused by the bathymetry of the Piovego river and the presence of algae and other marine life. At these frequencies, wind-driven waves would be the most relevant source of noise, especially given the closeness to the water surface; however, the environment does not present strong winds and the river is placid. Potential noise from air bubbles expelled by algae should be investigated.

The experiment was therefore repeated in the afternoon. This time the second modem was placed on a small boat, positioned between the two central pillars of the river: this way there was a more direct line of sight between the two hydrophones, which limited the self-interference; the maximum depth of the river was also exploited. The distance between transmitter and receiver was then only 10 m. It is safe to assume that any tested modulation that did not offer reception in our experiment would not work at any range, in this environmental conditions.

Figure 11: One of the two MODA devices used for the experiment. The board is connected to the battery and to the cable of the hydrophone.

Figure 12: The second modem was placed on a boat positioned between the wooden pillars.

With this setup, the results were much more satisfying.

3.3 Modulations

The modulations used belong to the group of PSK (*Phase Shift Keying*): the symbols used are waves shifted by a specific fraction of π, depending on the modulation. If n is the number of desired symbols, then $\delta = 2\pi/n$ is the phase shift of the wavefront. The value of n is a power of 2, and can range from 2 to 128. Each symbol can carry $b = \log_2(n)$ bits of information. When the value of n gets larger, it is possible to transmit data faster, but it also becomes more challenging to distinguish the symbols from each other, thus requiring a greater SNR to interpret the data. In this experiment we limited ourselves to $n = 2$ and $n = 4$, corresponding to the binary and quadrature phase shift keying, respectively. Since the latter one performed quite poorly in many of the observed tests, it would have been useless to try to employ finer modulations.

Two other parameters were significant in each test run. The first one is the samples-per-symbol (SPS) value. A higher amount of audio samples determines a longer symbol duration in the time domain, thus making it simpler to correctly interpret it at the receiver's end. However, requiring a lot of samples for each symbol slows down the transmission, so the aim should be to employ the lowest SPS value that ensures a reasonable PDR.

The second parameter is the presence or absence of the OFDM (Orthogonal Frequency-Division Multiplexing) modulation. When it is active, multiple subchannels are present, each with a slightly shifted carrier frequency. The subchannels partially overlap, but since they are orthogonal, the interference is canceled out. One could use completely separated subchannels, but it would require a larger bandwidth to fit the same number of them.

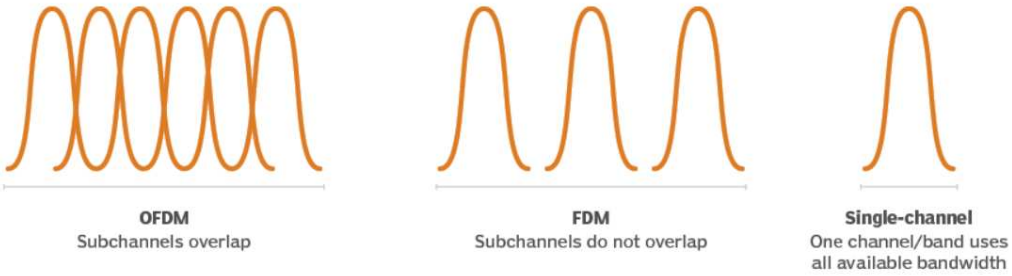

Figure 13: Visual representation of OFDM.

The use of OFDM allows to transmit multiple streams of data in parallel, making it possible to increase the bitrate. Alternatively, when a better reception is necessary, OFDM allows to increase the SPS value without affecting the bitrate.

When the OFDM is not employed, the term "FlexFrame" is used in the modulation: the modem's physical module has a FlexFrame wrapper, that allows for a quick switch between modulations.

3.4 Results

We will now illustrate the results of the experiment. We will analyze the most significant test runs, to deduce what types of modulation can be supported by the channel. In the following graphs, each dot represents a PDR calculated on a group of 10 packets. The groups are arranged in chronological order of transmission; each packet brings a payload of 31 characters, chosen from the alphabet (uppercase and lowercase) and the 10 digits, for a total of 62 possible symbols.

Firstly we tried a simple flex BPSK modulation, with a SPS value of 10:

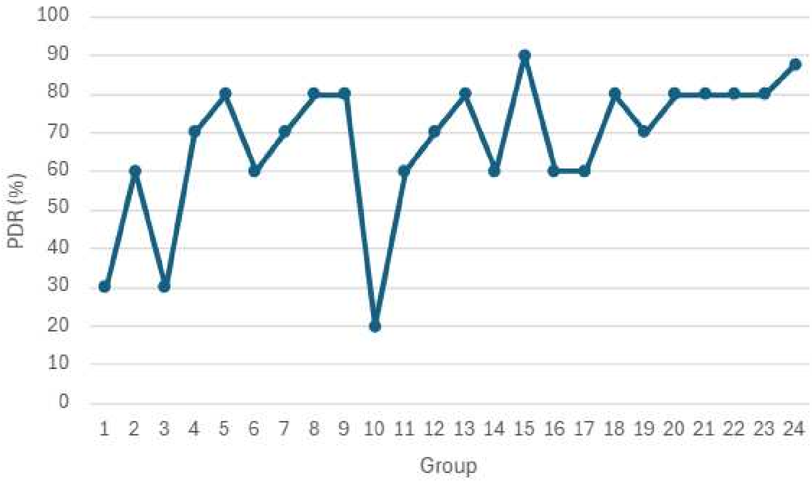

Figure 14: FlexFrame BPSK, 10 SPS. Overall reception is satisfactory.

After the first 40 packets, the PDR stays consistently above 60%. The overall average is 67.4%, which can be considered a success. The only exception is group 10, where the reception drops down to only 20%. Temporary drops like this can have many causes, among which the self-interference brought by temporary obstacles like fish or floating algae, or noise, such as the one produced by air bubbles.

Since this test was promising, we tried to lower the SPS value to achieve a higher bitrate. In the plot below, only 5 samples per symbol were taken.

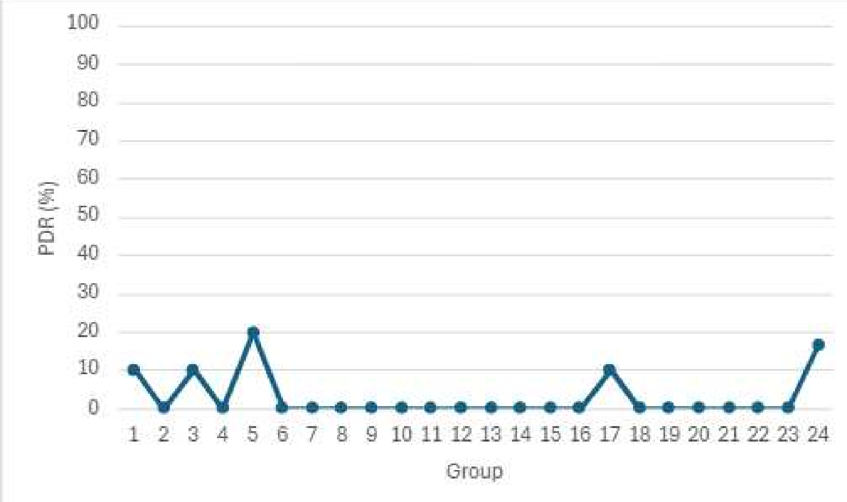

Figure 15: FlexFrame BPSK, 5 SPS. Reception is scarce

As we can see, 5 SPS are not enough to correctly receive the symbols: the average PDR is a mere 2.8%. In this case it is appropriate to perform a binary search to find the lowest SPS value that could ensure an acceptable reception. A value of 9 was the only one which saw more than half of the packets (specifically 52.8%) correctly received.

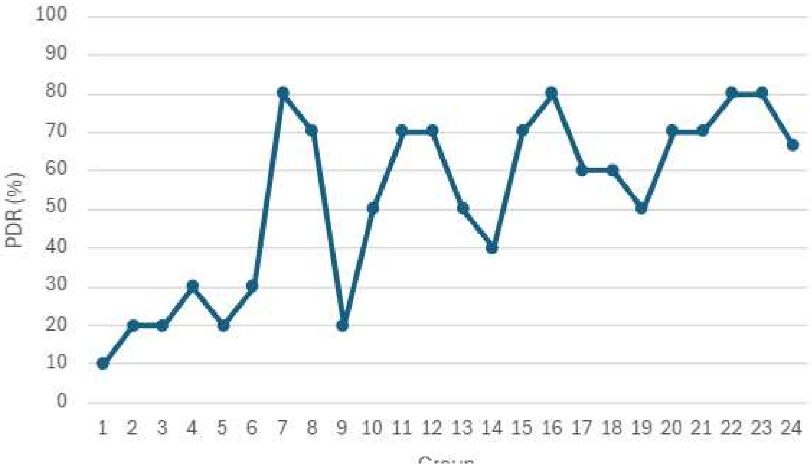

Figure 16: FlexFrame BPSK, 9 SPS. After a slow start, packet reception increases.

One can notice that the PDR visibly increases after the first 60 packets; a longer run will be needed in the future, and would probably lead to a better overall result.

We then switched to QPSK. This is a finer modulation, so we expected it would require more samples in order to be effective. At first we ran a test at 15 SPS:

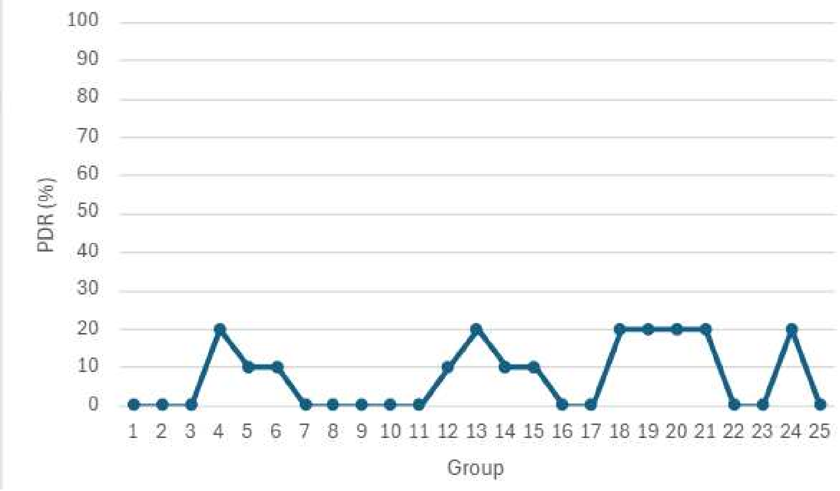

Figure 17: FlexFrame QPSK, 15 SPS.

The average PDR of 7.6% was definitely scarce. Setting the SPS value to 20, results slightly improved, even though they were still not quite satisfactory:

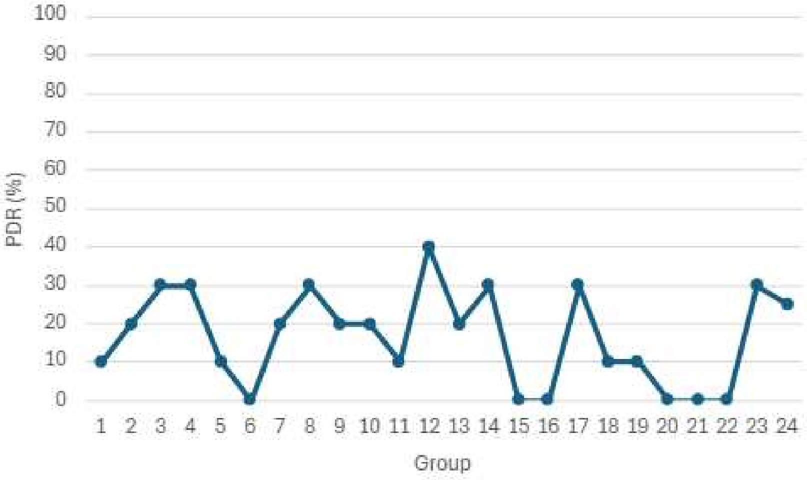

Figure 18: FlexFrame QPSK, 20 SPS.

Even by doubling the samples used for the BPSK case, we can see that the reception is quite low, with an average of just 16.5%.

From the transmitter's point of view, with a QPSK at 20 SPS, the datarate is the same as a BPSK at 10 SPS: a QPSK wave carries 2 bits instead of 1, but it is sampled twice as slowly as a BPSK one. Since the reception is much higher with the 10 SPS BPSK, this ought to be the preferred modulation.

The next plot refers to the first test run employing OFDM modulation. At 20 SPS BPSK, this shows results comparable to the flex 10 SPS BPSK, albeit still not reaching its performance.

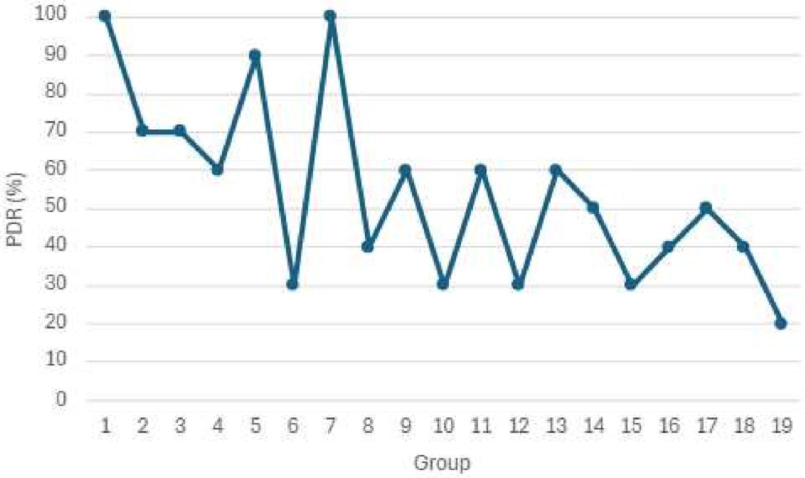

Figure 19: OFDMFlexFrame BPSK, 20 SPS.

With an average PDR of 54.2%, this can be considered a success. We tested the reception with 15 SPS, and subsequently with 17 SPS. In both cases, approximately one out of four packets were correctly received. The plot below shows the 17 SPS case, with an average reception of 25.5%.

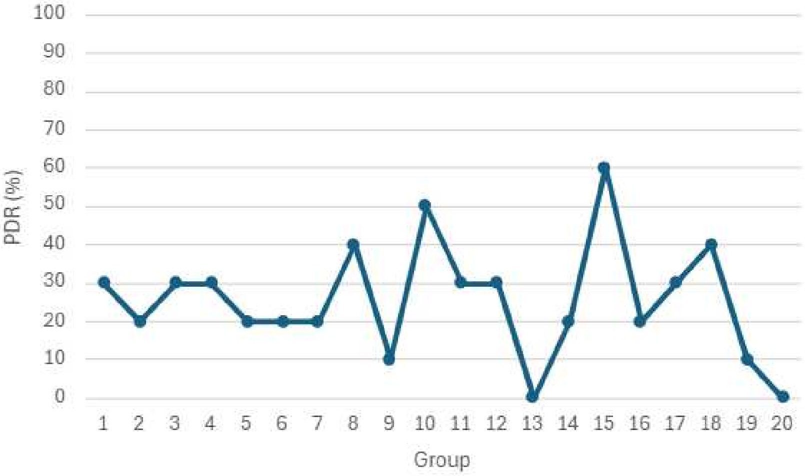

Figure 20: OFDMFlexFrame BPSK, 17 SPS.

Lastly, a OFDMFlexFrame QPSK at 20 SPS test run was performed. This solution was ineffective, with a packet reception of just 6.7%.

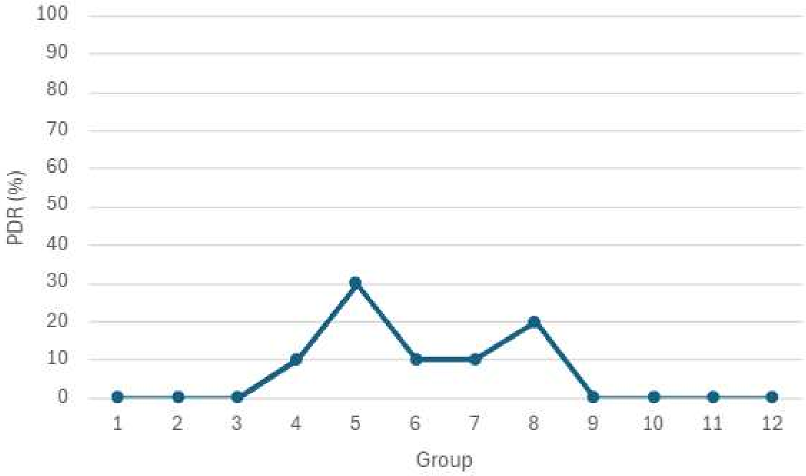

Figure 21: OFDMFlexFrame QPSK, 20 SPS.

4 Conclusions and future work

Research in underwater wireless communication still offers numerous challenges and opportunities. As the monitoring of marine wildlife, water biochemistry and natural disasters becomes of vital importance, new studies are needed to harness the possibilities of acoustics, optical and RF communication. Each of these technologies has unique characteristics: acoustics is best suited for long range communication, to exchange commands rather than complex data. On the other hand, RF can be used as a last-meter link, having a very short range but a high bitrate. Optical links can extend their reach further than RF, still supporting high speed transmission, but require a line of sight and certain illumination conditions. Therefore, employing nodes with multimodal hardware and software capabilities seems to be a promising solution, as it makes possible to compensate the respective shortcomings of each technology.

Running simulations within the DESERT framework, we showed the range and the depth achievable in different channel conditions, for simple scenarios involving two or three nodes, employing the aforementioned modes of transmission.

The experiment in the Piovego river, which was focused on close range acoustic transmission, suggests that a BPSK modulation at a sampling rate of 10 SPS yields the best results in terms of packet reception ratio, although a similar performance can be achieved with a OFDM BPSK modulation at 20 SPS. It is likely that the results would be different with an environment not as challenging as the Piovego river, which as we mentioned presents lots of self-interference due to the shallow riverbed. In any case, further tests need to be performed, preferably in winter, in order to have less algae that could constitute a barrier for the sound wave.

References

[1] A. Zoksimovski, D. Sexton, M. Stojanovic, and C. M. Rappaport, *"Underwater electromagnetic communications using conduction - channel characterization"*, Ad Hoc Networks, vol. 34, pp. 42-51, 2015.

[2] B. Shihada, O. Amin, C. Bainbridge, S. Jardak, O. Alkhazragi, T. K. Ng, B. Ooi, M. Berumen, and M.-S. Alouini, *"Aqua-fi: Delivering internet underwater using wireless optical networks"*, IEEE Communications Magazine, vol. 58, no. 5, pp. 84-89, 2020.

[3] *"Develogic Subsea Systems"*, http://www.develogic.de/

[4] M. Stojanovic, *"On the relationship between capacity and distance in an underwater acoustic communication channel"*, ACM Mobile Comput. and Commun. Review, vol. 11, no. 4, pp. 34-43, Oct. 2007.

[5] A. Pal, F. Campagnaro, K. Ashraf, R. Rahman, A. Ashok, H. Guo, *"Communication for Underwater Sensor Networks: A Comprehensive Summary"*.

[6] S. M. T. Islam and A. Ashok, *"Empirical characterization of vertical channel in underwater visible light communication"*, in 2019 14th International Conference on Underwater Networks and Systems (WUWNET), Oct 2019.

[7] T. Komine and M. Nakagawa, *"Fundamental analysis for visible-light communication system using led lights"*, IEEE Transactions on Consumer Electronics, vol. 50, no. 1, pp. 100-107, 2004.

[8] H. M. Oubei, C. Shen, A. Kammoun, E. Zedini, K.-H. Park, X. Sun, G. Liu, C. H. Kang, T. K. Ng, M.-S. Alouini, and B. S. Ooi, *"Light based underwater wireless communications"*, Japanese Journal of Applied Physics, vol. 57, no. 8S2, 2018.

[9] P. A. Forero, S. Lapic, C. Wakayama, and M. Zorzi, *Rollout algorithms for data storage- and energy-aware data retrieval using autonomous underwater vehicles*, in Proc. ACM WUWNet, Rome, Italy, Nov. 2014.

[10] S. Han, Y. Noh, R. Liang, R. Chen, Y.-J. Cheng, and M. Gerla, *Evaluation of underwater optical-acoustic hybrid network*, IEEE China Communications, vol. 11, no. 5, pp. 1518-1547, May 2014.

[11] F. Campagnaro, F. Favaro, F. Guerra, V. S. Calzado, M. Zorzi, and P. Casari, *Simulation of multimodal optical and acoustic communications in underwater networks*, in Proc. MTS/IEEE OCEANS, Genova, Italy, May 2015.

[12] R. Francescon, F. Campagnaro, F. Favaro, F. Guerra, M. Zorzi, *Software Defined Underwater Communications: an Experimental Platform for Research.*

[13] "HiFiBerry DAC+ ADC Pro," Available: https://www.hifiberry.com/shop/boards/hifiberry-dac-adc-pro

[14] E. Coccolo, F. Campagnaro, D. Tronchin, A. Montanari, R. Francescon, L. Vangelista, M. Zorzi, *"Underwater Acoustic Modem for a MOrphing Distributed Autonomous Underwater Vehicle (MODA)"*